Journal of Physics: Conference Series **141** (2008) 012019 doi:10.1088/1742-6596/141/1/012019

Applications of Ionization Spectroscopy to Study Small Bio-Molecules

Feng Wang[1]
Centre for Molecular Simulation, Swinburne University of Technology, P. O. Box 218, Hawthorn, Melbourne, Victoria, 3122, Australia

E-mail: fwang@swin.edu.au

Abstract. Ionization potential provides a useful quantum mechanical diagnostic for the oxidative potential of a molecule. However, to accurately predict the ionization binding energy spectra for even small biomolecules using relatively simple models is still a challenge in theoretical spectroscopy. In the progress report, recent progresses targeting core and valence binding energy spectroscopy of small bio-molecules, such as amino acids and DNA/RNA bases and their fragments, are discussed using density functional theory based models.

1. Introduction

The demands for gas phase information arise from the anticipation that many biological phenomena can be traced to the fundamental properties of molecular constituents. Intrinsic properties of bio-molecules, which are usually hidden in the complex medium of a real biological system, can be understood in an isolated environment in gas phase. Experiments in gas phase lead to large amounts of data, which provide insight into the physico-chemical origin of properties of biological molecules [1-5]. Both laser spectroscopy and computational modelling have significantly contributed to elucidating the structures and dynamics of these biomolecules and their solvated complexes in the gas phase [3-4, 6-13]. When a photoabsorption process occurs in biological systems such as living cells, it may cause certain photobiological effects on the system. Repairable and/or unrepairable changes, or damages, may cause macroscopic changes such as cell death or mutation in the biological systems. Initiating processes are clearly the same as those studied in atomic physics or photochemistry [14]. In a recent near-edge X-ray absorption fine structure (NEXAFS) spectroscopic study, it was found that gas-phase and condensed systems show more or less similarities in their fragment-ion yield curves [15].

Accurate prediction of ionization spectra of biomolecules has been a challenge for theoretical spectroscopy. Core-shell information was largely ignored in the past a few decades, such as the applications of the frozen core model. Quantitative treatment of NEXAFS spectra for even small bio-molecules such as amino acids [16] and DNA bases [17-19] are not fully understood. Experimentally, energy source or resolution of the techniques resulting in congested spectra has limited one's capability for more detailed understanding. For example, a photoelectron spectroscopic (PES) study of butan-2-ol gives only two peaks separating the C-H carbons and the C-OH carbon, thus Rennie et al [20] concluded that the C1s levels of buta-2-ol are not sensitive to molecular conformations. In contrast, in their recent experiment on substituted propane, $CH_3CH_2CH_2X$, Thomas et al [21] indicated that the C1s levels are indeed affected by the conformations. Theoretically, calculations far from trivial are

[1] To whom any correspondence should be addressed.

necessary to accurately reveal inner-shell properties and simple models such as Hartree-Fock (HF) are unable to reveal subtle differences caused by various chemical environment and conformation of bio-molecules. As a result, simple means are employed. For example, in a spectral analysis of L-alanine, a simple mean was employed to estimate the ionization potentials (IPs) from a pair of B3LYP and HF calculations without any rigorous scientific basis [22].

Valence-shell ionization spectra have been studied more extensively [23]. The reasons include (a) valence shell orbitals (such as frontier orbitals) of a molecule change relatively more significantly than core orbitals in the species and in chemical reactions, (b) good agreement with the experiment achieved from relevantly well developed models, such as the outer valence Green's function (OVGF) model and even the simple HF model, and (c) experimental accessibility. However, the energies of a molecule are usually more sensitive to radial displacements rather than angular displacements in the development of quantum chemistry in coordinate space. Energy differences among conformers of a bio-molecule can be subtle, when the conformers are dominated by angular changes. For example, pseudorotation produced conformers of the sugar moiety of DNA/RNA, tetrahydrofuran (THF), exhibit only subtle energy differences, which could not be conclusively differentiated in both experiments and theory for a long time [24-27]. There is no simple model which is the best for conformations of biomolecules so that various properties which are sensitive to particular conformers are readily employed, which makes a variety of methods detecting conformers. Some of the examples include dipole moments [28], quadrupole moments [29] and vibrational transition moments [30]. More recently, the symmetry of the HOMOs for THF conformers [25] and orbital momentum distributions of adenine [5,31] have been discovered as useful means to identify conformers of angular dependence.

In the present report, we present briefly our recent work in application of ionization spectroscopy to study biomolecules.

2. Computational details

Ionization spectra of molecules are transitions between ground electronic state and core hole (ionized) states or valence hole (ionized) states, respectively. Relevant energies between associated states determine the accuracy of the predicted spectral band positions in the binding energy spectra, and the wave functions (orbitals), in part, are responsible for the spectral band intensities. In the present study, all single point calculations are based on the optimized geometries, which are carried out using the B3LYP/aug-cc-pVTZ, B3LYP/TZVP and B3LYP/6-311++G** models incorporated in the Gaussian03 [32] or Gamess [33] computational chemistry packages, followed by vibrational analysis. The obtained geometries of the species exhibit minimum energies without any virtual frequencies.

For the binding energy spectra, single point calculations using density functional theory (DFT) based LB94/et-pVQZ model [34-35] and SAOP/et-pVQZ [36] are then employed to produce the core and valence orbital energies, respectively. The orbital ionization potentials (IPs) are approximated using the "meta"-Koopman's theorem [45] without further modification and scaling. The binding energy spectra are produced using density of states (DOS). A Lorentzian shape function with a uniform full width at half maximum (FWHM) is employed for all heavy (non hydrogen) atoms in the core shell. A different FWHM for valence shell is used. The DFT single point calculations are performed using the Amsterdam Density Functional (ADF) computational chemistry package [37]. The valence orbital momentum distributions (MDs) are calculated using electron momentum spectroscopic (EMS) method [38-39]. The orbital MDs are simulated via a Fourier transform using the HEMS program [40-41] (perfect-resolution EMS cross-sections).

3. Results and Discussion

3.1 Inheritance of DNA/RNA bases from parent pyrimidine and purine in the core shell

The simulated inner-shell N1s and C1s binding energy spectra of adenine (A) are compared [42] with a recent synchrotron sourced experimental spectra in gas phase [4], which is given in Figure 1. The agreement between the observed X-ray photoelectron spectra (XPS) in gas phase [4] and simulated spectra [42] makes this simple method very attractive. The LB94/et-pVQZ model is therefore, applied to calculate the IP spectra of other DNA/RNA bases in the present work.

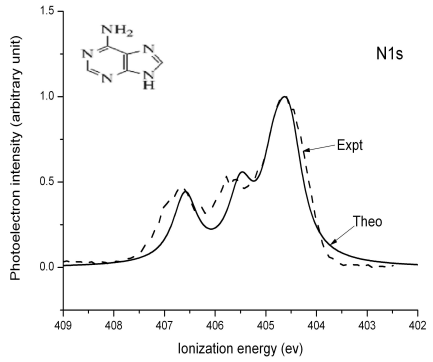

Figure 1(a). Comparison of the simulated (LB94/et-pVQZ) adenine N1s spectra (shifted by 1.65 eV, FWHM of 0.59 eV) with XPS [4].

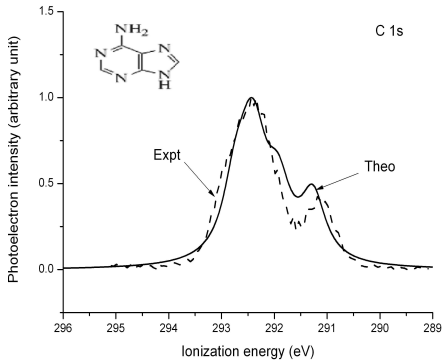

Figure 1(b). Comparison of the simulated (LB94/et-pVQZ) adenine C1s spectra (shifted by 0.85 eV, FWHM of 0.57 eV) with XPS [4].

Figure 2 provides the simulated C1s spectra of the pyrimidine (Py) bases (U, T, C and Py from the top to the bottom). Apparent site dependent changes with respect to the parent Py are observed. The C1s spectra of U and T, due to the two C=O groups at C(2) and C(4) positions, exhibit significant expansion to the larger energy end of the spectra, whereas the C1s spectrum of cytosine shows limited energy expansion. However, the degree of chemical shift of all C1s sites with reference to the parent pyrimidine, does not engage with any level crossings in the C1s spectra of the Py bases, but shifts reflecting the chemical environment of a particular C1s site in the bases. The most significant change in the C1s spectra of the pyrimidine bases is the elimination of equivalency of C(4) and C(6) sites in Py, due to the substitution of the C(2)-H bond by the C(2)=O bond in the Py bases.

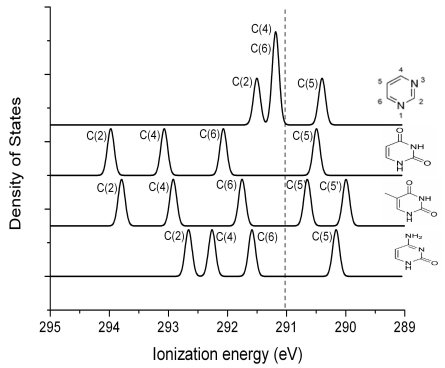

Figure 2. Simulated C1s inner-shell spectra of the pyrimidine bases, U, T and C with respect to the parent pyrimidine.

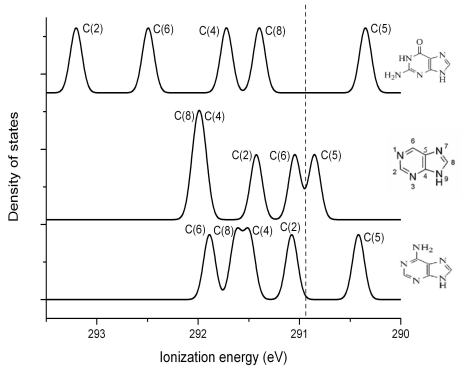

Figure 3. Simulated C1s inner-shell spectra of the purine bases, A and G with respect to the parent purine.

The N1s and C1s site dependent IPs of the double ring purine (Pu) bases have changed more significantly than the single ring Py counterparts, as the spectra of the Pu bases are not only associated with the spectral peak shifts, but also the site dependent energy level crossings [42]. Figure 3 provide the simulated C1s spectra of guanine (G), adenine (A) and their parent purine (G, Pu and A from the top to the bottom). In fact, when the resolution (FWHM = 0.136 eV) of the high resolution spectrum of adenine in figure 3 (bottom panel) reduces to a lower resolution, such as the XPS experiment resolution of FWHM = 0.57 eV [4], the adenine spectrum (bottom panel) of figure 3 becomes figure 1(b). The two spectra look different but only with a matter of resolution. The apparent changes in the C1s spectrum of G with respect to Pu are (a) the splitting of C(5) site from the rest of the C1s sites in A and G, and (b) the expansion of C1s spectral band, ranging from 1.17 eV in Pu to 2.85 eV in G, due to the significant blue shift of the C(2) and C(6) sites in G (see Figure 3). The C(2) site connected with the amino ($-NH_2$) attachment shifts more significantly than the C(6) site associated with the C=O attachment in G. The peak positions in G are very different from its parent Pu, too. For example, the IP energy order of the C1s sites in Pu is C(5)<C(6)<C(2)<(4)<C(8), whereas this order in G is given by C(5)<C(8)<C(4)<C(6)<C(2). There is little similarity in the two C1s spectra of A and G. As a result, in Figure 3 the IP energy peak in the lower end of the spectra can be separated from other C atoms of G and A than Pu.

In summary, the inner-shell spectral shifts of the bases with respect to their parent Py and Pu are single ring and double ring related. In the Py bases, when the derivatives such as U, T and C are produced, the chemical environment of the sites alters noticeably, leading to apparent spectrum rang expansions towards the blue energy end, depending on the bonding situation. The degrees of the site dependent shift in Py bases do not vary significantly, as no level crossings in the N1s and the C1s spectra are found. The C1s energy order of Py has been inherited and passed into the C1s spectra of U, T and C. The Pu bases exhibit a very different nature, however. With respect to the N1s and C1 spectra of the parent Pu, adenine inherits certain features in the N1s spectra as previously found [4] but little has been inherited by G [42]. In conclusion, if the DNA/RNA bases have more or less spectral and structural properties inherited from their parent Py and Pu species, G is the species with the least inheritance from its parent Pu in the inner shell.

3.2. The chemical picture of fragments in molecules: core and valence

Many biologically relevant molecules have their basic skeleton as an aromatic ring with a short alkyl or alkylamine side chain. As a result, information regarding the building block fragments is very useful to understand residues. In proteins, the smallest and most abundant aromatic residue is L-phenylalanine (Phen-X). Recent data mining exercises have shown that amide-aromatic interactions of phenylalanine are very important in the stabilization of protein residues over large configurational spaces [43]. Structurally, L-phenylalanine can be considered as one of the hydrogen atoms of benzene being replaced by L-alanine. It is useful if one could determine which fragments are responsible to an orbital or a group of orbitals in both core and valence space approximately, and which orbitals are responsible to the interactions. Such the knowledge of fragments in bio-molecules will largely enhance rational drug design and protein structures.

Table 1 gives the site specific binding energies in the core shells of the three species. The benzene core shell contains 12 electrons occupying four orbitals in which the 1e orbitals are doubly degenerated, due to the high symmetry of D_{6h}. When L-phenylalanine is produced, the benzene ring is distorted and the high symmetry exists no more. As a result, the orbital degeneracy of benzene loses in both core and valence shells.

Table 1. Site specific core ionization potentials (IPs) in the ground electronic states calculated using the LB94/et-pVQZ model (eV).

Atom site	IP(Benzene) C_6H_6		IP (L-alanine) $CH_3CH(NH_2)COOH$		IP (L-phenylalanine) $C_6H_5CH_2CH(NH_2)COOH$	
O-C			536.55	$(1a)^2$	535.85	$(1a)^2$
O-H			534.95	$(2a)^2$	534.37	$(2a)^2$
N-H_2			402.87	$(3a)^2$	403.73	$(3a)^2$
C-OOH			293.41 (295.3)#	$(4a)^2$	293.06	$(4a)^2$
Cα**			291.18 (292.3) #	$(5a)^2$	291.51	$(5a)^2$
C-H_2			289.76 (291.2) #	$(6a)^2$	290.10	$(6a)^2$
C-ben	289.502 (290.2)*	$(1a_{1g})^2$			290.04	$(7a)^2$
C-ben	289.498	$(1e_{1u})^4$			289.75	$(8a)^2$
C-ben	289.498				289.72	$(9a)^2$
C-ben	289.490	$(1e_{2g})^4$			289.66	$(10a)^2$
C-ben	289.490				289.65	$(11a)^2$
C-ben	289.486	$(1b_{1u})^2$			289.57	$(12a)^2$

*Expt. See [44].
#Expt. See [22].
**Cα represents the carbon atom which connects with four different groups, i.e., the chiral C atom, in L-alanine and L-phenylalanine

Figure 4 (a) gives the core binding energy spectra of canonical L-phenylalanine (X^1A), L-alanine and benzene, which are simulated using the DFT-LB94/et-pVQZ model (FWHM of 0.15 eV). The core binding energy spectral patterns of Phen-X and L-alanine are very much alike, indicating that Phen-X and L-alanine possess similar core frame, whereas the inner-shell binding energy spectrum of benzene seems "degenerated". However, a further study into the core shell of the three species in the range of ca 289-291 eV, it reveals that the benzene single band consists of 1,2,2,1 folds of four levels as given in Figure 4(b).

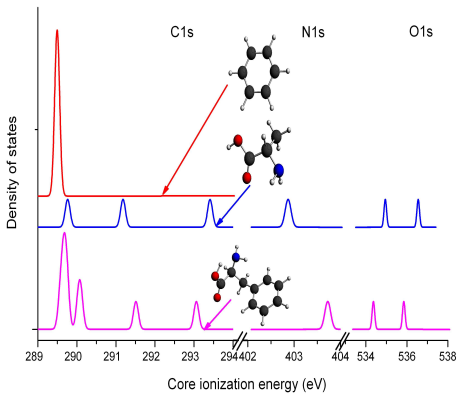

Figure 4(a). Simulated core binding energy spectra of benzene, L-alanine and L-phenylalanine.

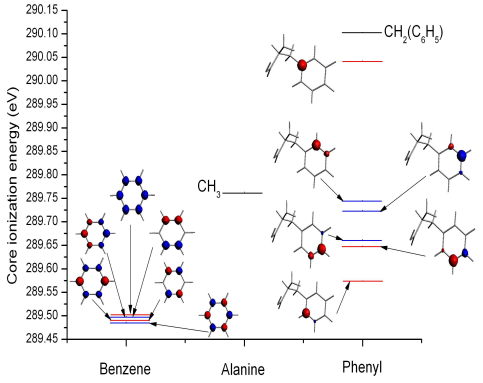

Figure 4(b). C1s energy levels of benzene, L-alanine and L-Phen-X in the region of 289-291 eV.

It is seen in Figure 4 that (a) L-phenylalanine indeed "mimics" the core shell structure of L-alanine, and the phenyl fragment can be treated as a functional group; (b) interactions between the L-alanine and phenyl fragments contribute to the apparently binding energy split, producing an energy band of the phenyl fragment of Phen-X at about 289-291 eV due to the symmetry reduction in the phenyl ring; and (c) chemical shift in the core shell indeed provides some useful information related to the subtle changes in the chemical environment of a particular element.

In valence space, the interaction of fragments and atoms are more intensive, so that the valence levels become more difficulty to separate into orbitals of fragments within a molecule. However, a single biomolecule could contain more than one functional group. For example, L- phenylalanine contains the phenyl and alanine functional groups as shown in the core shell. As a result, the valence orbitals of Phen-X are approximately divided into alanine related (group I), phenyl related (group II) and mixed (group III) orbitals [6]. Figure 5 (a) provides a representative orbital theoretical momentum distributions (TMDs) in group I, orbital 22a for alanine and orbital 40a for Phen-X. The orbital TMDs in Figure 5 (a) indicate that the phenyl fragment does not show sufficient impact on this alanine dominant orbital and its π-like bonding character. Figure 5 (b) shows that a doubly degenerated benzene orbital, $3e_{2g}$, splits into two orbitals of 38a and 39a in Phen-X, as a result of the symmetry reduction. The orbital TMDs and electron density distributions of the four related orbitals in this figure, clearly demonstrate the phenyl fragment in L-phenylalanine. Therefore, amino acids are not only important as building blocks of life, but also provide important information for us to understand basics in chemical science such as chemical bonding mechanisms and reaction dynamics.

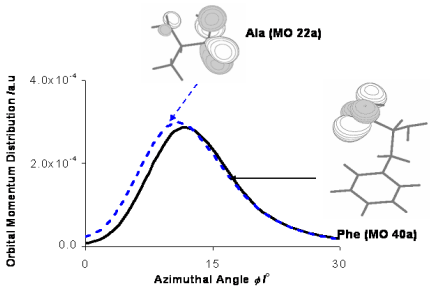

Figure 5(a). TMDs of orbitals 22*a* of alanine and 40*a* of phenylalanine*.

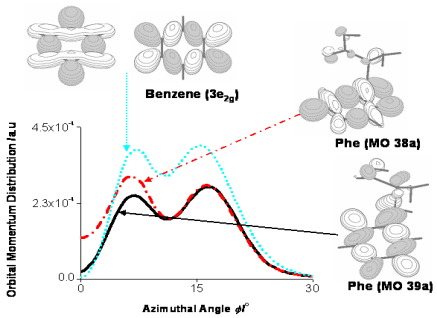

Figure 5(b). The doubly degenerated orbital $3e_{2g}$ of benzene, which splits into two orbitals of 38*a* and 39*a* in phenylalanine*[*].

3.3. Pseudorotation of tetrahydrofuran (THF): the HOMO

The phenomenon of pseudorotation has been a challenge as a lot of information needs comprehending. Conformations of THF, which are flexible along the pseudorotation path as a function of the pseudorotation angle ϕ, have haunted structural chemists for many years. Ambiguous experimental and theoretical results were obtained. For example, the most stable or the most populated conformer of tetrahydrofuran (THF) has been an open question for a long time. Conformers of THF at the local energy minima can be achieved through sugar puckering (pseudorotation) without across of large energy barriers. As a result, species containing the sugar moiety, such as nucleosides and nucleotides, present very flexible structures associated with various properties. The orbital symmetry does not conserve among the conformers produced by pseudorotation [26]. Until very recently, Yang et al. [25] concluded the most populated conformation of THF in gas phase is C_s, jointly using experimental and theoretical EMS. In that study, the symmetry of the highest occupied molecular orbitals (HOMOs) of conformer Cs is observed using the orbital momentum distributions (MDs). This section concentrates on the HOMO of THF, as a function of the pseudorotation angle ϕ.

[*] Azimuthal angle is related to momentum (in a.u.) as [39],

$$p = \left[(2k_s \cos\theta - k_0)^2 + 4k_s^2 \sin^2\theta \sin^2\left(\frac{\varphi}{2}\right) \right]^{\frac{1}{2}}.$$

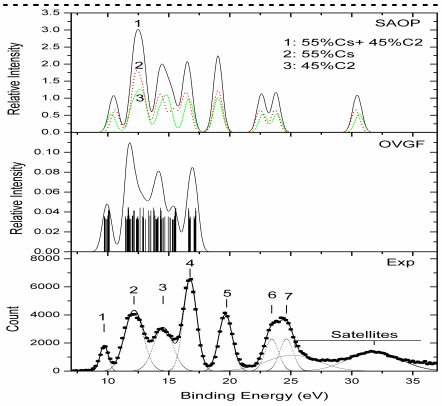

Figure 6(a). Binding energy spectra of THF: experiment and theory [27].

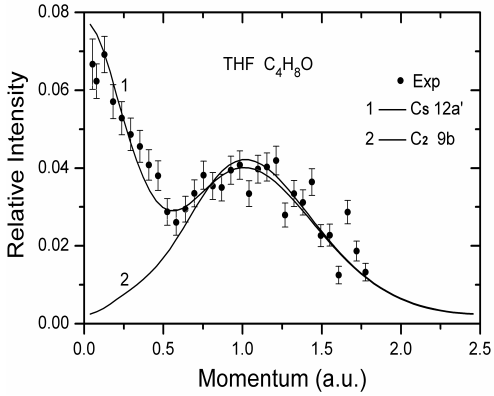

Figure 6(b). The HOMO MDs of THF-determination of the most populated conformer [25].

The observed valence binding spectrum of THF, given in Figure 6(a), is compared with the simulated ones. In the simulation, the Green function based OVGF/6-31G model and DFT based SAOP/et-pVQZ model [35-36] are employed. As found in [25-27], the HOMO of THF plays a particularly important role in pseudorotation of THF. The TMDs of the HOMOs of the C_s and C_2 conformers reveal significant different symmetries in their obitals, which identify the most populated conformer of THF [25] see Figure 6(b). The orbital MDs of the HOMOs are further simulated as a function of the pseudorotation angle ϕ. The simulated orbital MDs are presented in the region of [0º, 180º] with an interval of 15º [27]. Figure 7(b) exhibits the changes of the momentum distributions in the low momentum region of $p < 0.75$ a.u. The cross sections (the inserted in Figure 7(b)) at any given momenta, $p < 0.75$ a.u., form an asymmetric υ-shaped curve: the MDs decrease as the pseudorotation angle increases (ϕ<90º) and reach the minimum at ϕ=90º, then pick up as the pseudorotation angle ϕ (ϕ>90º) continues to increase. The chemical bonding mechanism is changing with the pseudorotation angle ϕ in THF. For example, the orbital is an $s^x p^y$-hybridized [46-47] when the pseudorotation angle ϕ=0º or 180º, that is, the C_s conformer (see Figure 7(b)). The s-electron component of the HOMO is reducing to reach the minimum, when the pseudorotation angle ϕ approaches 90º. At ϕ=90º (i.e., C_2 conformer), the orbital MDs then exhibit a bell-shaped distribution, indicating the p-electron dominated bonding.

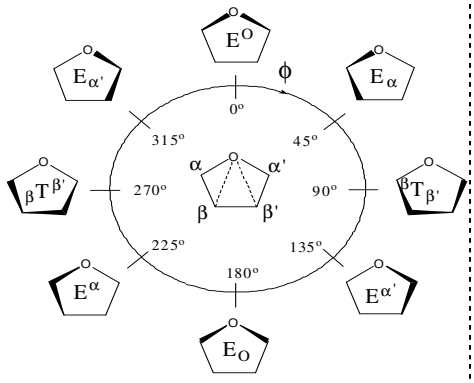

Figure 7(a). The pseudorotation wheel of tetrahydrofuran [26]

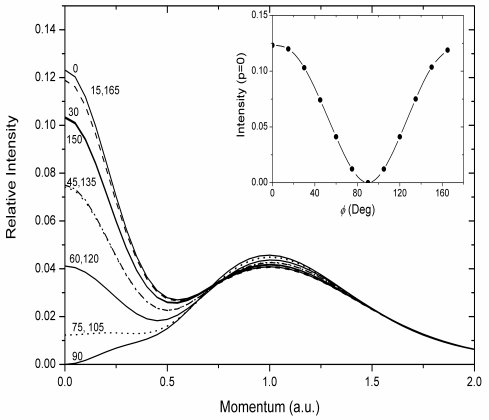

Figure 7(b).The HOMO MDs of THF as a function of the pseudorotation angle [27].

4. Conclusions

Ionization spectroscopy provides a close link between structure, function and measurement, with significant information of molecular orbital theory and chemical bonding mechanism. It is also a rich information source for core and valence electronic structures of bio-molecules. Methods applicable to small molecules are hardly generalized into larger bio-molecules, since properties such as bioactivity of larger bio-molecules may behave quite differently from small molecules. Accurate methods applicable to bio-molecules are limited, since the size of bio-molecules will saturate computing resources rapidly at this high level of theory. The demand of accuracy for bio-molecules is apparent due to their engagement with conformers. However, in the valence shell, the large number of valence orbitals quickly pushes the valence orbitals from discrete energy levels into energy bands, leading to a number of useful models such as ADC(4) and OVGF becoming prohibited. A number of conformations may be populated under the ambient conditions, so that the measured binding energy spectra can be congested, which further complicates the spectral analyses. The present study explores novel and simple methods to estimate building blocks of life to assist experimental measurements, in order to understand properties of larger species. The ultimate goal is to study larger nucleosides [11,48-49] which are important in life and medicinal sciences.

5. Acknowledgments

I would like to thank Vice-Chancellor's Research Award at Swinburne University of Technology for the recognition of the work done. The Australian Partnership for Advanced Computing (APAC) should be acknowledged for the award under the Merit Allocation Scheme and Swinburne University Supercomputing Facilities are also acknowledged for their support.

I sincerely wish to thank my collaborators for their support and contribution in this report as I have been "standing on the shoulders of Giants". In particular, the contributions from Dr. C. T. Falzon, Dr. C. G. Ning, Dr. Q. Zhu, Dr. P. Duffy and Mr. S. Saha are greatly appreciated.

6. References

1. Sponer J E, Sychrovsky V, Hobza P. and Sponer J 2004. *Phys. Chem. Chem. Phys.* **6** 2772.
2. Segala M, Takahata Y and Chong D P 2006 *J. Mol. Struct. (THEOCHEM).* **758** 61.
3. Saha S, Wang F, MacNaughton J B, Moewes A and Chong D P 2008 *J. Synch. Rad.* **15** 151.
4. Plekan O, Feyer V, Richter R, Coreno M, de Simone M, Prince K C, Trofimov A B, Gromov E V, Zaytseva I L and Schirmer J 2008 *Chem. Phys.* **347** 360.
5. Wang F, Downton T and Kidwani N 2005 *J. Theor. Comput. Chem.* **4** 247.
6. Wang F 2007 Computational Methods in Sciences and Engineering, Theory and Computation: Old Problems and New Challenges, 1, Maroulis G and Simos T *AIP Conference Proceedings*, 54.
7. Fujii K, Akamatsu K, Muramatsu Y and Yokoya A 2003 Nucl. *Instr. And Meth. in Phys. Res. B.* **199** 249.
8. Fujii K, Akamatsu K and Tokoya A 2004 *J. Phys. Chem. B.* **108**, 8031.
9. Li X, Bowen K H, Haranczyk M, Bachorz R A, Mazurkiewicz K, Rak J and Gutowski M 2007 *J. Chem. Phys.* **127**, 174309.
10. Wang F 2005 *J. Mol. Struct (THEOCHEM)* **728** 31.
11. Wang F 2006 *Macro. & Nano. Letters.* **1,** 23.
12. Falzon C T and Wang F 2005 *J. Chem. Phys.,* **123,** 214307.
13. Jones D B, Wang F, Winkler D A and Brunger, M J 2006 *Biophys. Chem*. **121** 105.
14. Usami N, Kobayashi K, Maezawa H, Hieda K, Ishizaka S,1991 *Int. J. Radiat. Biol.* **60** 757.

15. Ikeura-Sekiguchi H, Sekiguchi T, Saito N and Suzuki I H 2001 *J Synchrotron Rad* **8** 548.
16. Mochzuki Y, Koide H, Imamura T, Takemiya H 2001 *J Synchrotron Rad*. **8** 1003.
17. Harada Y, Takeuchi T, Kino H, Fukushima A, Takakura K, Hieda K, Nakao A, Shin S and Fukuyama H 2006 *J. Phys. Chem. A*. **110** 13227.
18. MacNaughton J, Moewes A and Kurmaev E Z 2005 *J. Phys. Chem. B* **109** 7749.
19. Magulick J, Beerbom M M, Lahel B and. Schlaf R 2006 *J. Phys. Chem. B* **110** 2692.
20. Rennie E E, Powis I, Hergenhahn U, Kugeler O, Marburger S and Waston T M 2002 *J. Phys. Chem. A* **106** 12221.
21. Thomas T D, Saethre L J and Borve K J 2007 *Phys. Chem. Chem. Phys*. **9** 719.
22. Powis I, Rennie E E, Hergenhahn U, Kugeler O and Bussy-Socrate R 2003 *J. Phys. Chem. A*. **107** 25-34.
23. Close D M, Crespo-Hernandez C E, Gorb L and Leszcznski J 2008 *J. Phys. Chem. A* **112** 4405.
24. Rayón V M and. Sordo J A 2005 *J. Chem. Phys.* **122** 204303
25. Yang T C, Su G L, Ning C G, Deng J K, Wang F, Zhang S F, Ren X G, and Huang Y R 2007 *J. Phys. Chem. A* **111** 4927.
26. Duffy P, Sordo J A and Wang F, 2008 *J. Chem. Phys.* **128** 125102.
27. Ning C G, Huang Y R, Zhang S F, Deng J K, Liu K, Luo Z H and Wang F 2008, (submitted)
28. Nguyen T V and Pratt D W 2006 *J. Chem. Phys.* **124** 054317.
29. Filsinger F, Erlekam U, von Helden G, Kupper J and Meijer G 2008 *Phys. Rew. Lett*. **100**, 133003.
30. Dong F and Miller R E 2002 *Science* **298** 1227.
31. Fonseca-Guerra C, Bickelhaupt F M, Saha S and Wang F 2006 *J. Phys. Chem. A*. **110** 4012
32. Frisch M J et al 2004 Gaussian, Inc., Wallingford CT, Gaussian 03, Revision D.01.
33. Schmid M W et al. 1993 *J. Comput. Chem*. **14** 1347.
34. Van Lenthe E and Baerends E J 2003 *J. Comput. Chem.* **24** 1142.
35. Chong D P, Lenthe E, van Gisbergen, S J A and Baerends E J 2004 *J. Comp. Chem*. **25** 1030.
36. Schipper P R T, Gritsenko O, Van Gisbergen V S J A, Baerends E J 2000 *J. Chem. Phys.* **112** 1344.
37. Baerends E J, et. al. 2006 ADF2006.01; Theoretical Chemistry, Vrije Universiteit: Amsterdam, The Netherlands.
38. McCarthy I E and Weigold E 1991 *Rep. Prog. Phys*., **54**, 789.
39. Weigold E and McCarthy I E 1999 Electron Momentum Spectroscopy Kulwer/Plenum, New York.
40. Neville J J, Zheng Y and. Brion C E 1996 *J. Am. Chem. Soc.* **118** 10533.
41. Duffy P, Casida M E, Brion C E, and Chong D P 1992 *Chem. Phys.* 159 347.
42. Wang F, Zhu Q and Ivanova E 2008, *J. Synch. Rad.* (in press).
43. Duan G, Smith V H Jr and Weaver D F 2002 *Int. J. Quantum Chem*. **90** 669.
44. Celius U, 1974 *Phys. Scripta* **9** 133.
45. Gritsenko O V, Braıda B and Baerends E J 2003 *J. Chem. Phys* **119** 1937.
46. Wang F 2003 *J. Phys. Chem. A*, **107** 10199.
47. Wang F, Brunger M J, McCarthy I E and Winkler D A, 2003 *Chem. Phys. Letts* **382** 217.
48. Wang F 2007 *J. Phys. Chem. B* **111** 9628.
49. Thompson A, Saha S, Wang F, Tsuchimochi T, Nakata A, Iumamura Y and Nakai H, 2008 (submitted)